

STATE OF THE ART IN ELECTROMAGNETIC FIELD COMPUTATION

C W Trowbridge

Vector Fields Ltd, 24 Bankside, Kidlington, Oxon, OX5 1JE, UK.

ABSTRACT

This paper is concerned with the current status in the computation of static magnetic and electric fields as applied to the design of cyclotron magnets and associated equipment. There is growing requirement for 3-D solutions to complement the standard techniques of analogue methods and measurements. The basic field equations are presented followed by a fairly full treatment of a stable algorithm for their solution using the finite element method. Two examples are given where such computations have proved to be very useful in the design of cyclotrons, i.e. the joint Dutch-French AGOR project, and the Oxford Instrument medical machine OSCAR. Integral methods are also referred to with a discussion on their likely increased use, in the future, using parallel processors.

1. INTRODUCTION

Magnet builders are becoming increasingly dependent on computational techniques for the optimisation of crucial design parameters. This activity is wide-spread and is central to a broad range of electromagnetic devices—from small domestic consumer products to large power engineering installations—as well as the enormous range of high technology applications supporting industry and research. This paper is concerned with computational aspects of cyclotron design, but the core issues of predicting the magnetic and electric fields for assemblies of ferromagnetic, dielectric and conducting materials etc. are common to all these applications.

The paper will begin by reviewing the static field equations, but eddy current effects, and high frequency phenomena are ignored entirely. The latter, though of immense importance in the RF aspects of cyclotron design, is outside the scope of this paper. For a fuller examination of the current status of field computation generally, including eddy current effects, the reader should consult the proceed-

ings of the COMPUMAG series of conferences [1,2,3]. The main part of the review will be concerned with the numerical solution of static field problems using the finite element method with a special emphasis on the field cancellation problem, see section 2.3.1. This will be followed by some specific examples on the use of field computation for cyclotron design. The examples given are taken from the work of magnet designers who have used techniques with which the author is associated, and he therefore apologises for any bias there may be! This review will end with some information on recent work using parallel computers which should enable more complex designs to be computed in the future.

2. THE STATIC FIELD EQUATIONS

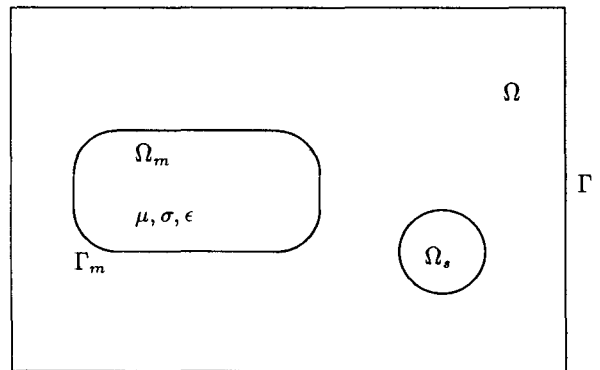


Figure 1: Model Problem for Static Fields

It is convenient to consider the elementary model problem (see figure 1) in which a volume of material Ω_m , with magnetic permeability μ , electrical conductivity σ , and electric permittivity ϵ bounded by a surface Γ_m , is immersed in a global volume of free space Ω bounded by a surface Γ which, furthermore, may be extended to infinity if required. The global region may also contain a number of prescribed sources Ω_s , which do not intersect Ω_m .

However care is needed if Ω contains multiply connected regions.

If time dependent effects are neglected then the field equations can be approximated by:

$$\nabla \cdot \mathbf{D} = \rho \quad (\text{Gauss's Law}) \quad (1)$$

$$\nabla \cdot \mathbf{B} = 0 \quad (2)$$

$$\nabla \times \mathbf{E} = 0 \quad (3)$$

$$\nabla \times \mathbf{H} = \mathbf{J}, \quad (\text{Ampere's Law}) \quad (4)$$

where $\mathbf{D}, \mathbf{B}, \mathbf{E}, \mathbf{H}$ are the usual field vectors, ρ and \mathbf{J} , the free charge and current densities respectively [4]. The field vectors are not independent since they are further related by the material constitutive properties;

$$\mathbf{D} = \epsilon \mathbf{E} \quad (5)$$

$$\mathbf{B} = \mu \mathbf{H}. \quad (6)$$

For current flow problems the current density in a conductor, \mathbf{J} , is given by:

$$\mathbf{J} = \sigma \mathbf{E} \quad (\text{Ohm's Law}). \quad (7)$$

In practice μ will often be field dependent, and furthermore, some materials will exhibit both anisotropic and hysteretic effects. The four field vectors must satisfy the following conditions at the interfaces between regions of different material properties;

$$(\mathbf{B}_2 - \mathbf{B}_1) \cdot \mathbf{n} = 0 \quad (8)$$

$$(\mathbf{D}_2 - \mathbf{D}_1) \cdot \mathbf{n} = 0 \quad (9)$$

$$(\mathbf{H}_2 - \mathbf{H}_1) \times \mathbf{n} = 0 \quad (10)$$

$$(\mathbf{E}_2 - \mathbf{E}_1) \times \mathbf{n} = 0. \quad (11)$$

2.1 Magnetic Vector Potential

Since the field vector \mathbf{B} satisfies a zero divergence condition, see equation (2), it can be expressed in terms of a vector potential \mathbf{A} as follows:

$$\mathbf{B} = \nabla \times \mathbf{A}, \quad (12)$$

and then, from equations (4,6) and (12), it follows that,

$$\nabla \times \frac{1}{\mu} \nabla \times \mathbf{A} = \mathbf{J}, \quad (13)$$

Is equation (13) sufficient? It is clear that for regions where the current density is zero the right-hand-side of equation (13) vanishes and the system is now not unique. In point of fact, it is necessary to specify the divergence (gauge) of \mathbf{A} and appropriate boundary conditions to ensure uniqueness. The commonest condition for static problems is the Coulomb ($\nabla \cdot \mathbf{A} = 0$) gauge [4].

2.2 The Two-Dimensional Case

The use of the magnetic vector potential for 2-D problems is widespread and for the very common limiting cases of infinitely long or axisymmetric models, where the current flows either parallel to the z - axis or in the azimuthal direction respectively, there will only be one component of \mathbf{A} involved. For the plane $x - y$ case this component is A_z , which will depend upon x and y only. Furthermore, by definition, A_z is now independent of the z coordinate and the Coulomb Gauge is automatically imposed, and from equation (13) A_z satisfies,

$$\nabla \cdot \frac{1}{\mu} \nabla A_z = J_z. \quad (14)$$

This formulation has been frequently used for cyclotron design when two-dimensional limits are a good approximation. Computer codes like TRIM [5], its derivative POISSON [6,7], and PE2D [8], for example, have proved indispensable tools for the magnet designer.

2.3 Scalar Potentials

All three static cases namely, magnetostatics, electrostatics and current flow can be solved in both two and three dimensions using scalar potentials.

2.3.1 Magnetostatics

The magnetic field \mathbf{H} can be partitioned into two fields namely, the field generated by the prescribed sources \mathbf{H}_s and the field arising from induced magnetism in ferromagnetic materials \mathbf{H}_m . Thus,

$$\mathbf{H} = \mathbf{H}_m + \mathbf{H}_s \quad (15)$$

and also since from equation (4) $\nabla \times \mathbf{H}_m = 0$ it follows that,

$$\mathbf{H} = -\nabla\phi + \mathbf{H}_s \quad (16)$$

where ϕ is called the reduced scalar potential [9], and by definition for conductor source regions with current density \mathbf{J}_s the source field is given by,

$$\mathbf{H}_s = \frac{1}{4\pi} \int_{\Omega} \mathbf{J}_s \times \nabla \left(\frac{1}{R} \right) d\Omega, \quad (17)$$

where $R = |\mathbf{r}' - \mathbf{r}|$ is the distance from the source point \mathbf{r}' to the field point \mathbf{r} , equation (17) is known as the Biot Savart Law [4].

In many cases, this can be integrated to give an analytic expression for H_s ; for complicated current paths, the expression can be integrated by a combination of analytic and numerical quadrature. The permanent magnet sources can be represented by a modified form of the constitutive relation, equation (6), of the form,

$$\mathbf{B} = \mu(\mathbf{H})(\mathbf{H} - \mathbf{H}_c) \quad (18)$$

where μ is a non-linear function of \mathbf{H} and is in general a tensor, and \mathbf{H}_c is the coercive field for the material [4].

In 'soft' magnetic materials, the coercive field intensity is normally assumed to be zero.

The governing equation for the reduced scalar potential, (ϕ), is obtained by taking the divergence of equation (18) ie.

$$\nabla \cdot \mu \nabla \phi = -\nabla \cdot \mu \mathbf{H}_c + \nabla \cdot \mu \mathbf{H}_s. \quad (19)$$

Whilst direct solutions of equation (19) are possible, in magnetic materials, the two parts of the field H_m and H_s tend to be of similar magnitude but opposite direction, so that cancellation occurs in computing the field intensity \mathbf{H} , giving a loss in accuracy [9,10]. This loss is particularly severe when μ is large. Fortunately, for regions where there are no conductor sources the total field \mathbf{H} can be represented by a scalar potential since, in this case, $\nabla \times \mathbf{H} = 0$ and it follows that,

$$\mathbf{H} = -\nabla\psi, \quad (20)$$

where ψ is known as the total scalar potential. The governing equation for regions without currents is given by,

$$\nabla \cdot \mu \nabla \psi = \nabla \cdot \mu \mathbf{H}_c \quad (21)$$

It is clear that the total scalar potential should be used to avoid cancellation errors, but unfortunately it cannot represent the whole problem, since in regions where there are currents this potential is multi-valued [4]. In a numerical algorithm however the two potentials can be combined to avoid the cancellation associated with reduced potentials and yet allow the inclusion of electric currents [10]. In regions that contain currents the reduced potential should be used, and elsewhere the total scalar potential. The solutions can be coupled at the interfaces of the regions by applying the continuity conditions equations (8) and (10), thus if region 1 contains all the ferromagnetic and permanent magnet sources and region 2 all the conductor sources then,

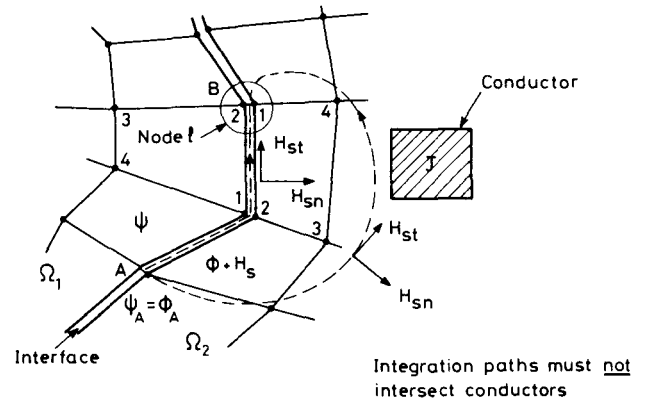


Figure 2: Source Scalar Potentials and Integration Paths

$$\mu_1 \left(-\frac{\partial \psi}{\partial n} - \mathbf{H}_{cn} \right)_1 = \mu_2 \left(\mathbf{H}_{sn} - \frac{\partial \phi}{\partial n} \right)_2 \quad (22)$$

$$\left(-\frac{\partial \psi}{\partial t} \right)_1 = \left(-\frac{\partial \phi}{\partial t} + \mathbf{H}_{st} \right)_2 \quad (23)$$

where \mathbf{n} and \mathbf{t} are the outward normal and tangent directions respectively. Equation (23) can be integrated over any path that does not intersect current regions to give an integral relationship between potentials at two points A and B, ie

$$\psi_B = \phi_B - \int_A^B \mathbf{H}_s \cdot d\mathbf{s}, \quad (24)$$

where \mathbf{H}_s is obtained explicitly from equation (17) and at point A, $\psi = \phi$, see figure 2.

2.3.2 Electrostatics

The electric field \mathbf{E} , defined by equation (3), can be ex-

pressed in terms of the electric scalar potential V as

$$\mathbf{E} = -\nabla V, \quad (25)$$

and from equation (1) V satisfies the Poisson equation

$$\nabla \cdot \epsilon \nabla V = -\rho. \quad (26)$$

2.3.3 Current Flow

In this case, if there are no sources or sinks of electric current inside the conducting region, the current density satisfies the divergence condition

$$\nabla \cdot \mathbf{J} = 0. \quad (27)$$

Hence from equations (7,25) the electric potential U satisfies

$$\nabla \cdot \sigma \nabla U = 0 \quad (28)$$

2.4 Numerical Solutions using Finite Elements

The equations (19,21,26,28) are all of the Poisson type and can be expressed generically as:

$$\nabla \cdot \mu \nabla \Phi = Q \quad : \quad \mathbf{r} \in \Omega \quad (29)$$

where Φ is a scalar potential, either reduced ϕ or total ψ subject to boundary conditions

$$\Phi = \bar{\Phi} \quad : \quad \in \Gamma_1 \quad (30)$$

$$\mu \frac{\partial \Phi}{\partial n} = \bar{p} \quad : \quad \in \Gamma_2 \quad (31)$$

where $\Gamma = \Gamma_1 + \Gamma_2$ on the surface of a domain Ω . The imposition of Equations (30) and (31) ensure that solutions to Equation (29) are unique. Following the standard finite element procedure of weighted residuals [11] the solution to equation (29) is approximated by a set of basis functions

$$\Phi \sim \bar{u} = \sum N_i u_i, \quad (32)$$

and by constructing a set of weighted residuals at each node of suitably chosen finite elements the residual is given by

$$\begin{aligned} R_i &= \int_{\Omega} W_i (\nabla \cdot \mu \nabla \bar{u} - Q) d\Omega \\ &+ \int_{\Gamma_2} \bar{W}_i \left(\mu \frac{\partial \bar{u}}{\partial n} - \bar{p} \right) d\Gamma + \int_{\Gamma_1} \bar{W}_i (\bar{u} - \bar{\Phi}) d\Gamma \\ &= 0 \end{aligned} \quad (33)$$

where the W_i , \bar{W}_i , and $\bar{\bar{W}}_i$ are an arbitrary set of weighting functions. It is necessary to use integration by parts to reduce the order of continuity required for the functions \bar{u} . In this case, integration by parts of the first term in the above equation gives;

$$\begin{aligned} \int_{\Omega} W_i (\nabla \cdot \mu \nabla \bar{u} - Q) d\Omega &= - \int_{\Omega} \nabla W_i \cdot \mu \nabla \bar{u} d\Omega \\ &+ \int_{\Gamma} W_i \mu \frac{\partial \bar{u}}{\partial n} d\Gamma - \int_{\Omega} W_i Q d\Omega \end{aligned} \quad (34)$$

and by choosing, $\bar{W}_i = -W_i$ to eliminate the normal gradient term along the boundary Γ_2 , Equation (33) becomes:

$$\begin{aligned} R_i &= - \int_{\Omega} \nabla W_i \cdot \mu \nabla \bar{u} d\Omega - \int_{\Omega} W_i Q d\Omega + \int_{\Gamma_2} W_i \bar{p} d\Omega \\ &+ \int_{\Gamma_1} W_i \mu \frac{\partial \bar{u}}{\partial n} d\Gamma + \int_{\Gamma_1} \bar{W}_i (\bar{u} - \bar{\Phi}) d\Gamma = 0 \end{aligned} \quad (35)$$

The Galerkin form [11] is chosen for the weighting functions in which W_i is identified with the basis functions, ie

$$W_i = N_i. \quad (36)$$

The Galerkin method leads to a symmetric system of equations and can be shown to be equivalent to the variational method [11]. As the N_i are functions, local to elements, containing the nodal parameter u_i , Equation (35) defines a set of algebraic equations based on the nodes. The boundary condition on Γ_1 is usually enforced and therefore the appropriate integrals are eliminated. The problem has now been reduced to the solution of a set of linear equations of the form:

$$K_{ij} u_j = C_i, \quad (37)$$

with

$$K_{ij} = \int_{\Omega} \nabla N_i \cdot \mu \nabla N_j d\Omega \quad (38)$$

the matrix K being sparse and symmetric for this particular choice of weighting functions. The right hand side vector C_i is given by:

$$C_i = \int_{\Omega} N_i Q d\Omega \quad (39)$$

In order to minimise the effects of field cancellation two regions are constructed as in figure 2. Each region can be subdivided into finite elements, except that the problem will now not be completely defined, since on the interface boundary Γ_l between the two regions both ψ and ϕ are unknown. This indeterminacy can be resolved by application of the interface conditions, Equations (23) and (24). For simplicity the contribution from hard magnetic materials (ie right-hand-side term in Equation (21)) will be omitted although it is perfectly straightforward to include these effects [10]. Applying the weighted residual method and integration by parts to each region independently,

$$R_1 = - \int_{\Omega_k} \nabla W_i \cdot \mu \nabla \psi d\Omega_k + \int_{\Gamma_l} W_i \mu \frac{\partial \psi}{\partial n} d\Gamma_l \quad (40)$$

and

$$R_2 = - \int_{\Omega_j} \nabla W_i \cdot \mu \nabla \phi d\Omega_j + \int_{\Gamma_l} W_i \mu \frac{\partial \phi}{\partial n} d\Gamma_l, \quad (41)$$

μ_2 has been removed, since it is constant in the region Ω_j from which it follows that the term containing H_s vanishes, since $\text{div}(\mathbf{H}_s) = 0$. The total residual is to be set to zero (i.e. $R_1 + R_2 = 0$), and by making use of the interface conditions (Equations (23) and (24)) the sum of Equations (40) and (41) become

$$\begin{aligned} & \int_{\Omega_k} \nabla W_i \cdot \mu \nabla \psi d\Omega_k + \int_{\Omega_j} \nabla W_i \cdot \mu \nabla \phi d\Omega_j \\ &= - \int_{\Gamma_l} W_i \left[-\mu \frac{\partial \psi}{\partial n} + \frac{\partial \phi}{\partial n} \right] d\Gamma_l \\ &= - \int_{\Gamma_l} W_i \mathbf{H}_s \cdot \hat{\mathbf{n}} d\Gamma_l. \end{aligned} \quad (42)$$

After applying the Galerkin method to Equation (43) with a finite-element discretisation, the coefficient matrix is identical to Equation (38) with appropriate permeability. At the interface Γ_l , either ψ or ϕ can be eliminated by Equation (24). Eliminating ϕ results in a right-hand side term for a node on the interface that is given by:

$$C = Kg - h \quad (43)$$

where K is the element matrix, Equation (38), and

$$g = \int_0^{t_1} H_{sn} dt \quad (44)$$

$$h = \int_{t_1}^{t_2} N_l H_{sn} dt, \quad (45)$$

see figure 2. The method described in this section is used in the 3-D code TOSCA [8].

2.5 Discussion on Field Cancellation

The use of combined potentials, reduced and total, have been recommended in order to minimize cancellation errors [9,10]. The effectiveness of single reduced potential methods depend critically on the sub-space of functions used to interpolate the coil fields \mathbf{H}_s , and in particular the relation between these functions and the finite element potential solution space. Implementations of the reduced potential method, Equation (19), usually use exact evaluation of \mathbf{H}_s at all points by analytic integration of the Biot-Savart expression for the field from a defined current distribution, Equation (17). To some extent the use of two potentials can be circumvented [12], albeit at a heavy computational cost. To achieve this the space of functions used

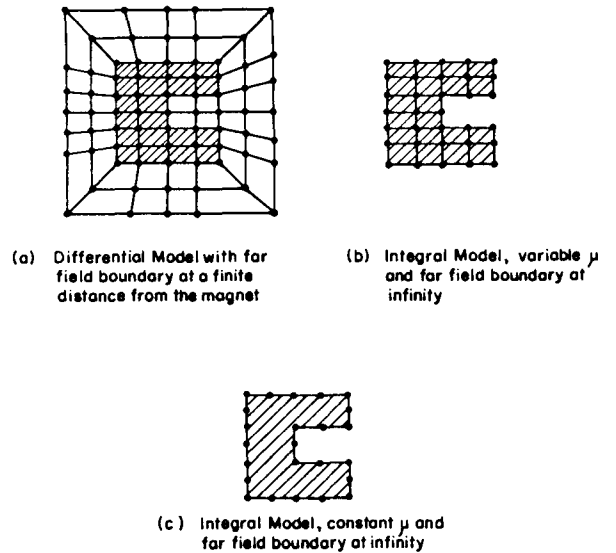


Figure 3: Integral versus Differential

to interpolate \mathbf{H}_s should be the same as that describing the gradients of the reduced potentials. If the two parts of the total field are not supported on the same space of functions then the cancellation between the two parts gives rise to large oscillations in the total field over each element.

Unfortunately the integration for \mathbf{H}_s is expensive for complex coils and when using a reduced potential method these integrations must be performed over the complete domain, whereas with the combined reduced and total potential

methods these values need only be evaluated in the reduced potential regions. Furthermore, using numerical basis function to support \mathbf{H}_s , implies that the elements must be capable of interpolating \mathbf{H}_s , with good accuracy.

3. INTEGRAL EQUATION FORMULATIONS

The integral equation forms of the governing field equations are often a viable alternative to the differential forms [13]. There are many different types that can be derived, see for example [13], however, in this paper, there is only enough space to quote the main equation types. For example, in magnetostatics the magnetisation vector \mathbf{M} satisfies a volume integral equation given by

$$\mathbf{M}(\mathbf{r}) = (\mu - 1) \left[\mathbf{H}_s(\mathbf{r}') - \frac{1}{4\pi} \nabla \int_{\Omega} \mathbf{M}(\mathbf{r}') \cdot \nabla \left(\frac{1}{R} \right) d\Omega \right]. \quad (46)$$

An alternative form using scalar potentials which is valid for linear materials only, and furthermore requires surface discretisation only is give by

$$\psi \mu = - \left(\frac{1}{4\pi} \int_{\Gamma} (\mu - 1) \psi \cdot \frac{\partial \left(\frac{1}{R} \right)}{\partial n} d\Gamma \right) + \psi_s. \quad (47)$$

Finally the classic boundary element method (BEM) first applied to mechanical problems [14] and later to electromagnetics [15] should be mentioned. The method is based on Green's theorem [4] to obtain solutions inside defined volumes in terms of surface values of potential and the normal derivative of potential. Thus, for 3-D linear problems the scalar potential at a point is given by

$$4\pi\phi = - \int_{\Gamma} \left(\frac{1}{R} \frac{\partial\phi}{\partial n} - \phi \frac{\partial \left(\frac{1}{R} \right)}{\partial n} \right) d\Gamma, \quad (48)$$

ie. given ϕ or $\frac{\partial\phi}{\partial n}$ on Γ , ϕ is uniquely defined in Ω . Problems with many regions with or without sources can be solved by applying equation (48) to each region simultaneously using total scalar potential ψ where there are no sources and the reduced potential ϕ elsewhere [15]. The additional equations required at the interfaces, where neither the potential nor its derivative are known, are supplied by the interface conditions as in equations (22,23).

4.1 Advantages of Integral Equations

The above equations are just three of the many forms that can be derived. The use of Integral methods for solving electromagnetic field problems has many advocates. The advantages (see figure 3) of integral formulations compared to the standard differential approach using finite elements are:

- (a) Only active regions need to be discretised which is an enormous advantage in 3D, see figure 3.
- (b) The far-field boundary condition is automatically taken into account by the formulation.
- (c) The fields recovered from the solution are usually very smooth since the local basis functions are proper field solutions.

Unfortunately, the computational costs are high and rapidly escalate as the problem sizes are increased. The use of parallel hardware to extend the range of the applicability of integral methods is considered in section 5.

4. Examples in AVR Cyclotron Design

A growing number of cyclotron designers are now using three-dimensional codes to help them optimise the critical parameters, see for example AGOR [16], OSCAR [17,18] in which the TOSCA code was used. Figure 4 shows the geometric model for the French-Dutch AGOR superconducting cyclotron. This is an example of a high energy machine (600MeV protons) to be used for physics experiments. Figure 5 shows axial field plots in the median plane ($z=0.0$) as a function of angle for several radii.

In the case of OSCAR, the 12 MeV superconducting cyclotron built by Oxford Instrument Ltd., UK for medical applications (Isotope production and tomography), several components were computed including the ion-source extraction system, the electrostatic inflector, and main magnet fields. Some statistics for these components are shown in table 1.

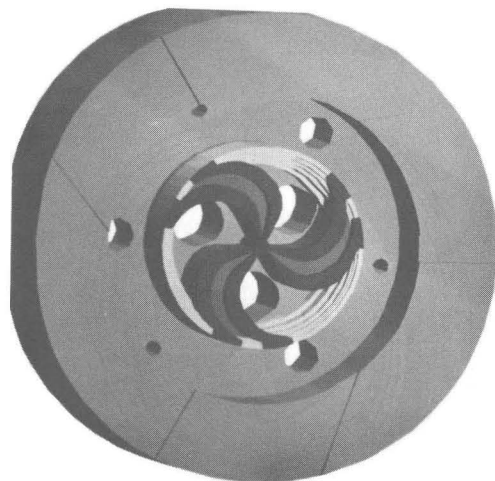


Figure 4: Geometric Model used in Computing AGOR

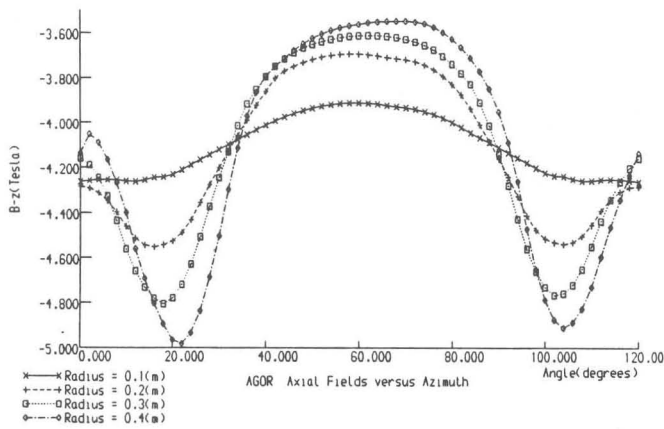


Figure 5: Computed Median Plane Fields in AGOR

In figure 6 a computer generated picture of the model used in the TOSCA code is shown. Full use was made of symmetry with a 60 degree sector actually analysed with implied symmetry by first reflecting in $y = 0$ plane and then repeating at 120 degrees. Computing the forces on the sectors turned out to be an important factor in the design, the results indicated that the webs supporting the sectors needed considerable stiffening.

In figure 7 the results for the average (over azimuth) computed and measured field as a function of radius are plotted. Also shown are the errors as a percentage. The maximum error is seen to be $\sim 1\%$, and it is possible that this would decrease by improving the material modelling, i.e. by measuring accurately the $\mathbf{B} - \mathbf{H}$ characteristics of the actual material used, also the model could be further refined to take account of fine details in the construction. Both these effects are important if very high accuracy is required. In figure 8 the mesh used in TOSCA for solving the electrostatic inflector is shown. The electrodes consist of a spiral channel which proved quite challenging to model, and, incidentally to visualize [17].

OSCAR Cyclotron Computer Statistics			
Component Problem	Code Nodes	C-Time(m) Acc. %	Remarks
Median Plane B_z	TOSCA 20000	270.0 0.5-1.0	Difficult geometry at small radii and variations in iron.
Magnetic Field along axis without sectors	PE2D 8000	4.0 0.3	Estimated Accuracy of measurement.
Injector Lens (Permanent Magnets)	PE2D 1000	5.0 1.0	Specified tolerance of Nd-Fe material.
Spiral Inflector	TOSCA 1000	10.0	Complex electrodes No measurements.

Table 1: The Oxford Instruments Ltd., Cyclotron OSCAR computed using VAX 8650.

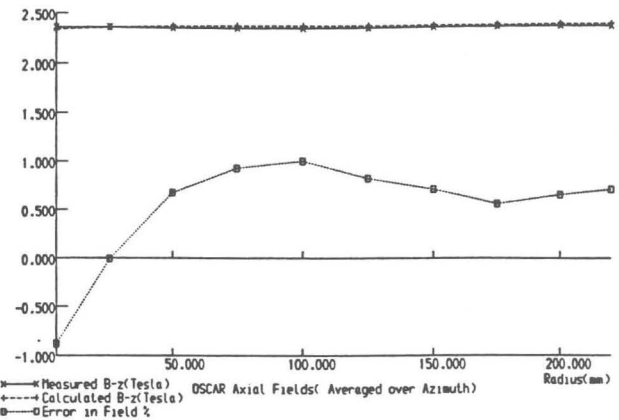


Figure 7: Field measurements compared with prediction

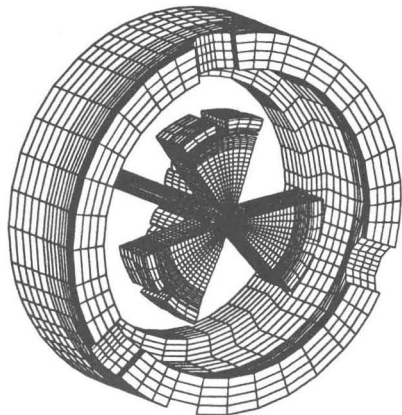


Figure 6: Geometry and Mesh for OSCAR

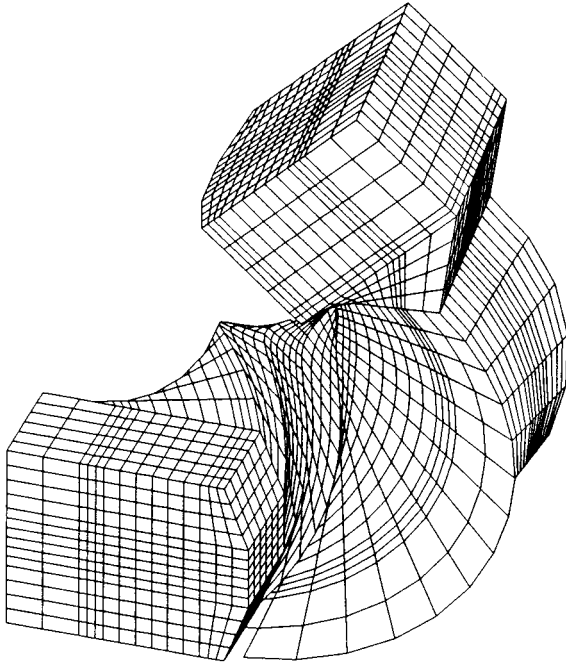


Figure 8: TOSCA mesh to analyse the OSCAR Inflector

5. Future Developments

The paper will conclude by listing a number of recent developments which should have some effect on the quality of cyclotron design.

5.1 The Impact of Parallel Processing

Parallel computing heralds a new vista for computational mechanics, or so we are told, but do the results bear any resemblance to the propaganda? There are two distinct types of hardware, the vector processor eg. FPS, and the loosely coupled massively parallel systems eg. Transputers. Some results follow for both types of system.

5.1.1 Solution speed-up on a Vector Processor [19]

Some speed-up times for running the TOSCA magneto-statics code on a Floating Point Systems M64/60 Vector processor are shown in table 2, the absolute times are in minutes. These results were obtained without the necessary re-coding in order to exploit more fully the vector machine. Some further benefits may be expected (A factor ~ 3) if this is done. In assessing these results it is essential to normalize the performance with the hardware costs which will of course be installation dependent. The effectiveness of using vector processing can be inferred

from the speed-up ratios shown in table 2. Thus, consider the timings for the OSCAR median plane fields(see table 1) which would be reduced from 270 minutes to 54 minutes(assuming the micro-vax2 is ~ 6 time slower than

From Scalar to Vector Processor			
Problem Nodes	Micro Vax 2	FPS M64/60 OPT=3	Ratio
400	1.600	0.060	27
18700	227.670	7.550	30
18700 non-linear	1375.73	40.530	34

Table 2: Speed-up statistics for TOSCA

the vax-8650). Furthermore, if vector optimised linear algebra is used, the computer time could be reduced to ~ 20 minutes.

5.1.2 Integral Methods and Parallel Processing

In section 3. integral equation formulations were briefly introduced and their strengths and weaknesses summarised. In solving a magnetostatic problem using boundary elements the following computational stages are performed:

- (a) *Source Fields* $\rightarrow n$ operations

$$\mathbf{H}_s = \int_{\Omega_c} \mathbf{J} Q d\Omega_c$$
- (b) *Matrix set-up* $\rightarrow n^2$ operations

$$A = \int_{\Omega} F d\Omega$$
- (c) *Solve Equations* $\rightarrow n^3$ operations

$$Ax = B$$

 Matrix A is fully populated

Of the above only item(c) is not a perfectly parallel operation i.e. containing both communication and calculation. In figure 9 some recent results for a solving a magnetostatic problem using arrays of transputer are shown [20] in which it can be seen that up the number of processors (32) good efficiency was obtained ($\sim 80\%$). This result is encouraging and it is likely that integral methods will become an important technique in the future as the use of parallel hardware becomes wide-spread, this especially attractive since relatively low cost systems involving transputer arrays can be constructed using small workstations as hosts.

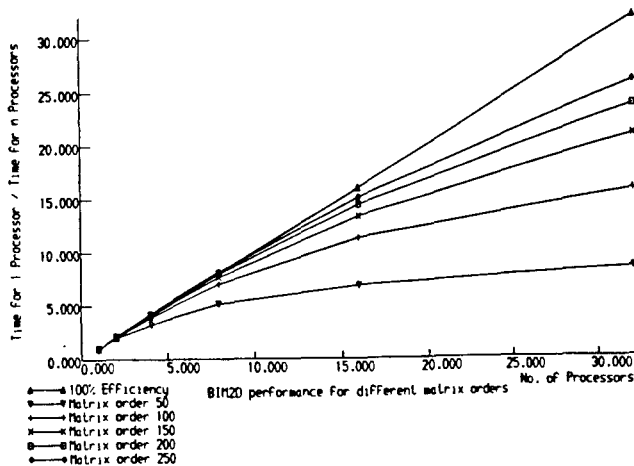


Figure 9: Using Transputers to speed up Integral Equation Solutions

5.2 The Design Environment

In recent years, the major emphasis on Computer Integrated Manufacture(CIM) research and development activity has been in the area of automatic manufacturing, where technical and economical feasibility is certainly critical for a viable CIM environment. Cyclotrons are complex devices that are difficult to design and manufacture so what impact will these recent developments have? In order to achieve a truly integrated manufacturing environment, it is necessary to integrate many activities into the design structure. In most cases, computer aided drafting tools are provided, but they are seldom connected in an integrated way to the design process and the dependent analysis tools are still only available via separate and frequently unrelated analysis codes. Possible ways of improving the situation include strengthening the robustness of analysis codes by error estimation, adaptive meshing and postprocessing features, and providing an effective integrated environment with drafting and design tools.

With the improvements available in analysis tools the task of the analyst can be made much simpler. However there is still the overriding difficulty that a realistic design needs to be analysed bearing in mind its coupled nature. Very few problems in reality can be analysed using tools based on a single discipline. For example in cyclotron devices, forces generated by the high magnetic fields effect the design. To model such a device accurately, it is necessary to analyse the same problem using both electromagnetic and stress-analysis tools. Ideally, the analysis should be carried out using a single, fully coupled model for whole problem, but this is still at an early stage of development. Some recent work has attempted to define a design environment which

should go some way toward integrating analysis packages and standard design procedures [21]. It is with such a system that designers can make best use of their time, and improve both their creativity and productivity.

ACKNOWLEDGEMENTS

The author would like to express his thanks to Marcel Kruip of Oxford Instruments Ltd., for his help in preparing this paper including the information relating to the OSCAR cyclotron computer models. He also thanks Hans Schreuder of KVI, Groningen, Holland for the information on the AGOR cyclotron.

References

- [1] W. Lord, ed., *Compumag Fort Collins Proceedings*, IEEE Trans Magnetics 21(6) 1985, 1985.
- [2] K. Richter, ed., *Compumag Graz Proceedings*, IEEE Trans Magnetics 24(1) 1988, 1987.
- [3] K. Miya, ed., *Compumag Tokyo Proceedings*, 1989. To take place September 1989.
- [4] J. A. Stratton, *Electromagnetic Theory*. New York: McGraw Hill, 1941.
- [5] A. A. Winslow, "Numerical solution of the quasi-linear poisson equation in a non-uniform triangular mesh," *J Comput Phys* 1, p. 149, 1971.
- [6] K. Halbach and R. Holsinger, "Poisson user manual," Tech. Rep., Lawrence Berkeley Laboratory, Berkeley, CA.
- [7] C. Iselin and R. Holsinger, "Program poisson," Tech. Rep. T604, CERN, Geneva, 1982.
- [8] *TOSCA, SCARPIA, OPERA, and PE2D User Manuals*. Vector Fields Ltd., 24 Bankside, Kidlington, Oxford OX5 1JE, 1988.
- [9] J. Simkin and C. W. Trowbridge, "On the use of the total scalar potential in the numerical solution of field problems in electromagnets," *IJNME*, vol. 14, p. 423, 1979.
- [10] J. Simkin and C. W. Trowbridge, "Three dimensional non-linear electromagnetic field computations using scalar potentials," *Proceedings of the IEE*, vol. 127, no. 6, 1980.
- [11] O.C.Zeinkiewicz, *The Finite Element Method*. Maidenhead, Berkshire, England: McGraw Hill, 1977.

- [12] J. Simkin, "Magnetostatic fields in 3-d," *VECTOR Electromagnetics Newsletter*, vol. 4, no. 2, 1988.
- [13] C. W. Trowbridge, *Applications of Integral Equation Methods for the Numerical Solution of Magnetostatic and Eddy Current Problems*. Chichester: Wiley, 1979.
- [14] M.A.Jaswon, "Integral equation methods in potential theory," *Proc. Roy. Soc. A*, 275, p. 23, 1963.
- [15] J.Simkin and C.W.Trowbridge, "Magnetostatic fields computed using an integral equation derived from green's theorem," in *Compumag Conference on the computation of magnetic fields*, (Chilton, Didcot, Oxon, UK), p. 5, Rutherford Appleton Laboratory, 1976.
- [16] H. Schreuder 1989. KVI, Groningen, Holland, Private Communication.
- [17] M. Kruip 1989. Oxford Instruments plc, Eynsham, Oxon, UK, Private Communication.
- [18] M.F.Finlan *et al.*, "A light, superconducting h^- cyclotron for medical diagnostics and neutron radiography," in *Eleventh International Conference on Cyclotrons and Their Applications*, (Kawada Building, Koishikawa 2-3-4, Bunkyo, Tokyo 112.), p. K26, Ionics Publishing Company, Ltd., 1987.
- [19] C.P.Riley, "Solution of em fields on vector processors," *VECTOR Electromagnetics Newsletter*, vol. 4, no. 1, 1988.
- [20] C.F.Bryant and C.W.Trowbridge, "Specification of the boundary demonstrator using transputers," Tech. Rep., Vector Fields Ltd., 24 Bankside, Kidlington, Oxford OX5 1JE, 1988. Esprit(1051), ACCORD/WP5/VFL/DEL/001/291.88/CWT Project Report.
- [21] G.Molinari *et al.*, "Integrating analysis and design," in *CIM EUROPE 5th Annual Conference*, (IFS Publications, 35-39 High St., Kempston, Bedford MK42 7BT, England, UK), 1989.